



## Original Research Article

### Elucidation of the Influence of Coal Properties on Coal –Char Reactivity: A Look at Southern Hemisphere Coals

**\*Odeh, A.O., Ogbeide, S.E. and Okieimen, C.O.**

Department of Chemical Engineering, Faculty of Engineering, University of Benin, PMB 1154, Benin City, Nigeria.

\*odehandy@yahoo.com

#### ARTICLE INFORMATION

##### Article history:

Received 08 July, 2018

Revised 17 September, 2018

Accepted 24 September, 2018

Available online 30 December, 2018

##### Keywords:

Oxygen combustion reactivity

Coal-char

Petrographic

Maceral content

Activation energy

#### ABSTRACT

*Pyrolysis is the first step in most coal conversion processes such as combustion, gasification and liquefaction. Coal char combustion is influenced by a wide variety of parameters (burnout time, heat release, mineral matter content etc.) which are factored into the reactivity of the char. Six coals of different ranks were subjected to conventional, advanced characterization and combustion reactivity experiments. The char reactivity exhibited the same trend of decrease with increasing pyrolysis temperature for the different coals evaluated at four combustion temperatures. The derived aromaticity, total reflectance, surface area and porosity were found to increase with increasing pyrolysis temperature. The activation energy of the various chars was also determined and a mean value of 184 kJ/mol for lignite, 154 kJ/mol for sub-bituminous, 94 kJ/mol for low volatile bituminous, 146 kJ/mol for high volatile bituminous, 113 kJ/mol for semi-anthracite and 152 kJ/mol for the anthracite coal respectively were obtained.*

© 2018 RJEES. All rights reserved.

## 1. INTRODUCTION

Coal conversion processes such as combustion, gasification and liquefaction are considered to take place in four stages or zone in a typical reactor, of which pyrolysis is the second zone. The pyrolysis zone impacts most coal conversion processes since it is the first chemical step and has an influence on subsequent stages. On heat treatment, the coal particles undergo thermo-chemical decomposition with liberation of volatiles and the formation char. The char reactivity is dependent on both the physical and chemical changes that results from heat treatment (Aarna and Suuberg, 1998). The physical changes include but not limited to softening, swelling, re-solidification, surface area, porosity of the solid material whereas chemical changes include bond breaking and recombination (Arenillas et al., 2003). The coal char structure is influenced not only by the properties of the parent coal, but also by the operating condition such as the heating rate (Bar-Ziv and Kantorovich, 2001), pressure (Beamish et al., 1998; Jones et al., 1999), the maximum temperature experienced (Kulaots et al., 2002) the residence time at this temperature (Kulaots et al., 2007) and the

gaseous atmosphere of the conversion process (Liu et al., 2000). Both variables (coal properties and process condition) contribute and influence the amount and nature of volatiles produced, as well as the rate (Sima-Ella et al., 2005). Many authors have examined the coal and char relationship to characterize coal and the resultant char to comprehend the rationale of the relationship between char reactivity's in combustion/gasification and char/coal chemical and physical properties (Kulaots et al., 2007).

Char reactivity is an important parameter that moderates the behavior of coal during combustion or gasification (Odeh, 2015). Among the techniques employed, the thermogravimetry analysis (TGA) technique is commonly used to quantify reactivity. In addition, thermogravimetry has the added advantage of readily showing the changes in reaction rate combustion/gasification as the reaction proceeds. In TGA, the weight of a char sample is determined as a function of time and temperature as it is subjected to a controlled temperature programme (Sima-Ella et al., 2005). TGA experiments are often performed isothermally, where the sample is heated to a constant temperature; or linearly heated; occurs at a constant rate Isothermal TGA is less convenient because of the excessive time and multiple experiments required but it has been found that the kinetic parameters obtained from this option are more valid than those from non-isothermal technique (Beamish et al., 1998)

Although much work has been conducted exploring coal pyrolysis (Odeh, 2015), extensive research on a definitive mechanism based on systematic and theoretical analyses on the thermal behavior and kinetics of the coal to char transition are seldom reported. Aarna and Suuberg (1998) investigated the influence of particle size and heating rate on pyrolysis characteristics and kinetics and reported that coal pyrolysis process is strongly affected by both heating rate and particle size. Also, there was an increase of activation energy with increasing coal particle size ( $< 0.075\text{mm}$ ) and decreasing heating rate at the pyrolysis temperature range of  $350 - 1300\text{ }^{\circ}\text{C}$ . Arenillas et al. (2003) conducted a comparative study on coal pyrolysis using both isothermal and non-isothermal techniques and reported that the non-isothermal technique presented less experimental difficulties and that values obtained for the kinetic parameters agreed with the literature. Jones et al. (1999) examined coal structure and reactivity changes induced by chemical demineralization on a bituminous coal and reported that the structural changes induced by the chemical treatment resulted in much better combustibility characteristics for the demineralized sample than those of the parent coal, together with a concomitant decrease in the emissions of sulphur dioxide. Liu et al. (2000) reported the influence of pyrolysis temperature on char optical texture and reactivity on ten coal of varying rank, the chars were prepared at temperatures of  $1000$  and  $1300\text{ }^{\circ}\text{C}$  and at a heating rate of  $25\text{ }^{\circ}\text{C}/\text{min}$ . The reactivity analysis was isothermal at  $500\text{ }^{\circ}\text{C}$  and they reported that the presence of inertinite derived materials in high rank coal chars enhanced their reactivities, whereas the opposite was observed for low rank coal chars. This could be attributed to the thermoplastic transformation evident in low rank coals yielding lower reactivity chars.

Here a systematic and a temperature programmed combustion of six southern hemisphere coals of different rank to investigate the coal to char transition was performed on a  $\leq 75\text{ }\mu\text{m}$  particle size coal chars prepared in a horizontal tube furnace at a heating rate of  $25\text{ }^{\circ}\text{C}$  from  $450$  to  $700\text{ }^{\circ}\text{C}$  at atmospheric pressure. Char reactivity were examined by  $\text{O}_2$  isothermal thermogravimetric analysis (TGA) technique to understand the coal to char transition in acid washed coals.

## 2. MATERIALS AND METHODS

### 2.1. Sample Preparation

Six coals of varying rank were used: a lignite coal from Germany (LIG); a sub-bituminous coal from Nigeria (SUB); two South African bituminous coals (one is low volatile bituminous (BIT-LV) and the other, high volatile bituminous coal (BIT-HV); South African semi-anthracite (SA); and anthracite from South Africa (ANT). The coal samples were pulverized to coal particle size of  $\leq 75\text{ }\mu\text{m}$  by employing a mechanical size reduction jaw crusher (Samuel Osborne (SA) LTD, model: 66YROLL) and a Fritsch P-14 rotary mill

containing ceramic balls (Model number: 46 – 126). The required particle size of  $\leq 75 \mu\text{m}$  was finally obtained from screening the particles from the rotary mill using a  $75 \mu\text{m}$  screen. All the samples were stored under argon in sealed bags. The prepared coal samples were acid washed by sequential leaching with hydrofluoric acid (HF) and hydrochloric acid (HCl) as detailed in Odeh (2015). The HF (48%) and HCl (32%) were obtained from Associated Chemical Enterprise (ACE), South Africa.

## 2.2. Apparatus and Procedure

The char production sequence: 40g of the acid-washed coal were devolatilized in a horizontal tube furnace at atmospheric conditions. The samples were flushed with nitrogen (AFROX, ultra high pure grade) for 15 minutes. at atmospheric conditions. A flow rate of 1 litre/min was used. The furnace was heated at  $20 \text{ }^\circ\text{C}/\text{min}$  to the target temperature, and held isothermal for 60 min. The target temperature ranged from 450 to  $700 \text{ }^\circ\text{C}$ .

The conventional chemical analyses (both proximate and ultimate analyses) and calorific value of the untreated coal, acid-washed and heat-treated samples were performed according to the ASTM 3172, ASTM 3176 and ISO 1928 standards respectively at Advanced Coal Technology (ACT), Pretoria, South Africa. The surface areas of the various samples were determined using the carbon dioxide ( $\text{CO}_2$ ) adsorption dubinin radushkerich (DR) method on a Micromeritics ASAP2020 surface area analyser. Prior to  $\text{CO}_2$  adsorption, the samples (about 0.20 g) were degassed under vacuum ( $10.0 \mu\text{mHg}$ ), at 25 and  $380 \text{ }^\circ\text{C}$  for 48 hours for both the coals and chars respectively. The evacuated sample was analysed at  $0 \text{ }^\circ\text{C}$  in an ice bath. The spectra used in obtaining the structural properties of both the coal and char were obtained from the fourier-transform infrared spectrometer equipped with an attenuated total reflectance (FTIR-ATR), model Perkin-Elmer Spectrum 400. The procedure of FTIR-ATR as detailed by Liu et al. (2000) was used.

Aromaticity ( $f_a$ ) was obtained from the ratio of aromatic bands in the  $900 - 700 \text{ cm}^{-1}$  region to the aliphatic and aromatic bands in the  $3000 - 2815 \text{ cm}^{-1}$  region. The total reflectance (contribution from both inertinite and vitrinite macerals) of the parent coals and chars indicating coal reflectance was obtained following the procedure and equipment at Coal and Carbon laboratory, University of Witwatersrand, South Africa detailed in Odeh (2015). The porosity and the pore size distribution of the coals and chars were performed at Council of Scientific and Industrial Research (CSIR), South Africa, using small angle X-ray scattering (SAXS), following the procedure and equipment at CSIR, Nano-Structured Materials Centre detailed in Kulaots et al. (2007).

Thermogravimetric analyses of the chars were carried in a Leco TGA701 thermogravimetric analyser with pneumatic carousel assembly with capacity of being loaded with 19 samples per run with a precision of  $\pm 0.02$ . The analyses were performed at Coal and Carbon laboratory, University of Pretoria, South Africa. The char combustion experiments were carried out isothermally at four different temperature ranging from 370 to  $415 \text{ }^\circ\text{C}$ . The samples were heated under nitrogen from ambient temperature to the target temperature for an hour, after weight stabilization the nitrogen was replaced by oxygen atmosphere (10 volume %) and held isothermal for six hours at a heating rate of  $10 \text{ }^\circ\text{C}/\text{min}$ . at atmospheric conditions. Samples mass of approximately 2g, with a particle size of  $\leq 75 \mu\text{m}$ , were used to reduce mass transfer effects. The selection of these experimental conditions was based on recommendations from researchers on the need for the samples to be distributed uniformly on the bed of the analyzer and not having a bed thickness  $> 1 \text{ mm}$ . The specific reactivity of the char was calculated by:

$$R = \frac{1}{W} \frac{dW}{dt} \quad (1)$$

Where W is the weight of the char dry ash-free basis (daf) at any given time time t. The intrinsic reactivity was obtained by normalizing the specific reactivity of the char by the DR micro-pore surface area obtained from the ASAP 2020 surface area analyzer (Kulaots et al., 2007).

### 3. RESULTS AND DISCUSSION

#### 3.1. Char Chemical and Physical Properties Analysis

Table 1 gives a comprehensive summary of detailed proximate, ultimate, calorific value, FTIR, DR surface area and total maceral analyses of the acid-washed coals, where coals are listed by increasing rank (lignite to anthracite) as determined by petrographic analysis (Odeh, 2015).

Table 1: Properties of acid-washed coal

| Coal                                | LIG  | SUB  | BIT-LV | BIT-HV | SA   | ANT  |
|-------------------------------------|------|------|--------|--------|------|------|
| Inherent moisture (air dried) wt. % | 1.7  | 1.9  | 1.3    | 2.7    | 2.3  | 2.5  |
| Ash (air-dried) wt. %               | 0.8  | 2.0  | 3.3    | 1.2    | 1.8  | 1.5  |
| Volatile matter (air-dried) wt. %   | 60.3 | 43.2 | 25.0   | 27.2   | 9.6  | 6.8  |
| Fixed carbon (air-dried) wt. %      | 37.3 | 53.0 | 70.4   | 68.9   | 86.3 | 89.2 |
| Carbon (daf) wt. %                  | 69.2 | 75.1 | 80.9   | 83.4   | 89.0 | 85.6 |
| Hydrogen (daf) wt. %                | 6.2  | 5.2  | 4.2    | 4.6    | 3.3  | 2.4  |
| Nitrogen (daf) wt. %                | 0.6  | 1.8  | 2.3    | 2.0    | 1.8  | 2.0  |
| Oxygen (daf) wt. %                  | 20.3 | 17.4 | 12.3   | 9.1    | 5.0  | 7.7  |
| Sulphur (daf) wt. %                 | 2.7  | 0.1  | 0.3    | 1.0    | 0.7  | 2.1  |
| Gross calorific value (MJ/kg)       | 28.9 | 29.3 | 30.0   | 32.0   | 33.3 | 32.7 |
| Total reflectance (Ro)              | 0.35 | 0.77 | 1.27   | 1.23   | 2.45 | 2.94 |
| H/C                                 | 1.08 | 0.83 | 0.62   | 0.66   | 0.45 | 0.34 |
| O/C                                 | 0.22 | 0.17 | 0.11   | 0.08   | 0.04 | 0.07 |
| $f_a$                               | 0.40 | 0.58 | 0.74   | 0.72   | 0.84 | 0.98 |
| Fuel ratio                          | 0.6  | 1.2  | 2.8    | 2.5    | 9.0  | 13   |
| DR surface area (m <sup>2</sup> /g) | 109  | 140  | 169    | 142    | 199  | 136  |

The chemical rank parameters follow the expected trend with increasing rank, meaning, a decrease in volatile matter, hydrogen content, oxygen content, atomic O/C ratio and atomic H/C ratio and an increase in carbon content, surface area, calorific value, fuel ratio and aromaticity (Sima-Ella et al., 2005). Some scatter in the atomic H/C and surface areas can be explained by variation in petrographic composition as can be seen in Table 2. The carbon content of the coals on dry ash free basis (daf) varies from 85.6 to 69.2 % for anthracite to lignite respectively. The atomic volatile matter on air dried basis varies from 6.8 to 60.3 % for anthracite to lignite respectively. The atomic H/C ratio decreases with increase in coal rank (1.08 for lignite and 0.34 for anthracite); atomic O/C ratio equally decreases with increase in coal rank (0.22 for lignite and 0.07 for anthracite). The aromaticity was found to increase with increasing coal rank (0.40 for lignite and 0.98 for anthracite). The same trend was obtained for the fuel ratio, that is, it increased with increasing coal rank (0.60 for lignite and 13 for anthracite). The micropore surface area equally exhibited increase with increasing coal rank but with variation with vitrinite-rich coals (coals containing more than 50 volume % of vitrinite content). The Coals SUB, BIT-LV and SA falls under this category of vitrinite-rich coals as can be seen in Table 2. The scatter in the surface area can be attributed to the effect of the acid-washing on the vitrinite macerals thereby increasing the active surface area and invariably the total surface area which could imparts on the reactivity of the coal. Vitrinite-rich coals have been considered to be more reactive than inertinite-rich coals as has been reported by other investigators (Bar-Ziv and Kantorovich, 2001). Table 2 gives a breakdown of the detailed petrographic analyses, where coals are presented in order of increasing rank (lignite to anthracite) with variation in petrographic composition.

Table 2: Petrographic characteristics of acid-washed coal

| Coal   | LIG                     | SUB                                   | BIT-LV                           | BIT-HV                           | SA                                      | ANT                           |
|--|-------------------------|---------------------------------------|----------------------------------|----------------------------------|---|-------------------------------|
| Rank   | Lignite –<br>low rank C | Sub-<br>bituminous<br>– low rank<br>B | Bituminous –<br>medium rank<br>C | Bituminous –<br>medium rank<br>C | Semi-<br>anthracite<br>– high<br>rank C | Anthracite<br>–high rank<br>B |
| Vitrinite reflectance<br>(% RoV)                                 | 0.30                    | 0.47                                  | 0.73                             | 0.78                             | 2.48                                    | 3.26                          |
| Total reflectance (%<br>Ro)                                      | 0.35                    | 0.77                                  | 1.27                             | 1.23                             | 2.45                                    | 2.94                          |
| Macerals analysis (mmfb)   |                         |                                       |                                  |                                  |   |                               |
| Reactive macerals  | 91.0                    | 71.8                                  | -                                | 48.0                             | -                                       | -                             |
| Coal vitrinite<br>content  | 34.0                    | 56.5                                  | 78.0                             | 32.0                             | 82.0                                    | 48.0                          |
| Coal liptinite content   | 39.5                    | 10.5                                  | 8.0                              | 6.0                              | -                                       | -                             |
| Coal total inertinite  | 24.0                    | 33.0                                  | 12.0                             | 60.0                             | 16.0                                    | 49.0                          |
| Visible minerals   | 1.5                     | -                                     | 2.0                              | 2.0                              | 2.0                                     | 3.0                           |
| Microlithotype analysis (vol. % mmb) - mono-macerals             |                         |                                       |                                  |                                  |   |                               |
| Vitrite %  | -                       | -                                     | 56                               | 9                                | 51                                      | 29                            |
| Inertite %   | -                       | -                                     | 14                               | 32                               | 18                                      | 41                            |
| Visible minerals - Organic/inorganic association (Carbominerite) |                         |                                       |                                  |                                  |   |                               |
| Maceral + clays +<br>quartz %                                    | -                       | -                                     | 6                                | 5                                | 10                                      | 7                             |
| Macerals + sulphide<br>%   | -                       | -                                     | 2                                | 2                                | 1                                       | 1                             |
| Macerals +<br>carbonates   | -                       | -                                     | 1                                | 1                                | 1                                       | <1                            |
| Mineral-rich particles - Minerite                                |                         |                                       |                                  |                                  |   |                               |
| Clay & quartz groups<br>%  | -                       | -                                     | 4                                | 4                                | 3                                       | 3                             |
| Sulphide group %   | -                       | -                                     | 3                                | 3                                | <1                                      | <1                            |
| Carbonate group  | -                       | -                                     | 2                                | 2                                | <1                                      | <1                            |

The vitrinite content of the macerals obtained exhibited no definite trend with the LIG having the least value of 34 vol. % and the SA the highest value of 82 vol. %. The inertinite content of the macerals obtained is 12 vol. % for BIT-LV with the least value and 60 vol. % for BIT-HV with the highest value. The liptinite content of the macerals obtained is 39.5 vol. % LIG; 10.5 % for SUB; 8 % for BIT-LV; 6 % for BIT-HV, while the two anthracitic coals, SA and ANT had no liptinite content. The visible mineral content obtained varies from 1.5 to 3 % for lignite to anthracite respectively. The presence of the minerals after the acid-washing process could be attributed to the organic/inorganic association in the coal matrix as can be seen in Table 2 under the carbominerite analysis. Clay minerals have been reported to be difficult to dissociate or separate from the organic/inorganic matrix (Beamish et al., 1998).

### 3.2. Coal to Char Transformation Evaluation

Table 3 gives an insight into the coal to char transformation. Results presented are in increasing coal rank (lignite to anthracite). The same trend as obtained for the parent coals was observed for the heat-treated coals (chars) for the obtained chemical analysis data, that is, the lowest temperature treated coals having the highest atomic H/C ratio, atomic O/C ratio compare to the high temperature treated coal.

Table 3: Derived properties of heat-treated coal (chars)

| Temperature (°C) | Porosity (%) | Ro (Vol %) | O/C  | H/C  | f <sub>a</sub> | FR   | DR (m <sup>2</sup> /g) | E <sub>a</sub> (kJ/mol) |
|------------------|--------------|------------|------|------|----------------|------|------------------------|-------------------------|
| LIG              |              |            |      |      |                |      |                        |                         |
| 450              | 13           | 1.26       | 0.10 | 0.45 | 0.66           | 1.9  | 285                    | 220                     |
| 500              | 16           | 1.79       | 0.08 | 0.40 | 0.69           | 2.2  | 323                    | 428                     |
| 550              | 25           | 2.28       | 0.05 | 0.28 | 0.73           | 2.3  | 381                    | 111                     |
| 600              | 30           | 2.75       | 0.03 | 0.28 | 0.74           | 8.8  | 414                    | 37                      |
| 650              | 22           | 3.65       | 0.03 | 0.21 | 0.76           | 13.3 | 451                    | 121                     |
| 700              | 15           | 4.36       | 0.02 | 0.13 | 0.79           | 21.0 | 475                    | 184                     |
| SUB              |              |            |      |      |                |      |                        |                         |
| 450              | 11           | 1.49       | 0.08 | 0.45 | 0.75           | 2.9  | 246                    | 347                     |
| 500              | 13           | 2.05       | 0.06 | 0.38 | 0.78           | 3.2  | 291                    | 137                     |
| 550              | 14           | 2.41       | 0.04 | 0.32 | 0.81           | 3.4  | 342                    | 190                     |
| 600              | 19           | 3.15       | 0.03 | 0.26 | 0.84           | 6.1  | 387                    | 32                      |
| 650              | 20           | 3.93       | 0.03 | 0.16 | 0.87           | 9.7  | 405                    | 57                      |
| 700              | 19           | 4.65       | 0.03 | 0.13 | 0.90           | 20.3 | 413                    | 166                     |
| BIT- LV          |              |            |      |      |                |      |                        |                         |
| 450              | 11           | 1.77       | 0.05 | 0.42 | 0.84           | 5.5  | 243                    | 172                     |
| 500              | 14           | 2.26       | 0.04 | 0.36 | 0.88           | 6.6  | 253                    | 163                     |
| 550              | 20           | 2.66       | 0.05 | 0.31 | 0.90           | 9.0  | 333                    | 58                      |
| 600              | 21           | 3.30       | 0.05 | 0.27 | 0.93           | 11.4 | 338                    | 90                      |
| 650              | 20           | 3.90       | 0.04 | 0.20 | 0.97           | 16.3 | 374                    | 44                      |
| 700              | 19           | 4.74       | 0.03 | 0.09 | 1.00           | 24.0 | 402                    | 37                      |
| BIT- HV          |              |            |      |      |                |      |                        |                         |
| 450              | 12           | 1.40       | 0.05 | 0.45 | 0.83           | 6.0  | 206                    | 487                     |
| 500              | 15           | 2.05       | 0.04 | 0.39 | 0.86           | 7.6  | 253                    | 143                     |
| 550              | 17           | 2.68       | 0.03 | 0.34 | 0.89           | 10.2 | 294                    | 71                      |
| 600              | 19           | 3.34       | 0.03 | 0.29 | 0.92           | 12.4 | 331                    | 25                      |
| 650              | 23           | 3.93       | 0.02 | 0.22 | 0.95           | 18.6 | 347                    | 29                      |
| 700              | 21           | 4.68       | 0.01 | 0.14 | 1.00           | 24.1 | 361                    | 118                     |
| SA               |              |            |      |      |                |      |                        |                         |
| 450              | 14           | 2.15       | 0.04 | 0.40 | 0.94           | 11.6 | 221                    | 239                     |
| 500              | 15           | 2.57       | 0.07 | 0.40 | 0.95           | 13.8 | 234                    | 62                      |
| 550              | 17           | 2.78       | 0.03 | 0.34 | 0.98           | 16.2 | 274                    | 104                     |
| 600              | 18           | 3.41       | 0.03 | 0.28 | 1.00           | 19.5 | 300                    | 59                      |
| 650              | 23           | 4.09       | 0.03 | 0.21 | 1.00           | 25.4 | 313                    | 84                      |
| 700              | 22           | 4.86       | 0.03 | 0.13 | 1.00           | 29.6 | 368                    | 130                     |
| ANT              |              |            |      |      |                |      |                        |                         |
| 450              | 11           | 2.56       | 0.03 | 0.31 | 0.97           | 16.5 | 210                    | 79                      |
| 500              | 14           | 2.91       | 0.03 | 0.28 | 0.98           | 16.8 | 218                    | 198                     |
| 550              | 15           | 3.28       | 0.03 | 0.28 | 1.00           | 19.7 | 221                    | 208                     |
| 600              | 16           | 3.59       | 0.03 | 0.25 | 1.00           | 20.3 | 241                    | 95                      |
| 650              | 21           | 4.29       | 0.03 | 0.22 | 1.00           | 24.5 | 262                    | 111                     |
| 700              | 17           | 4.79       | 0.03 | 0.13 | 1.00           | 27.8 | 263                    | 218                     |

f<sub>a</sub>=aromaticity; FR=fuel ratio; DR=DR surface area; \* % change; Ro=total reflectance

The atomic H/C ratio for lignite (LIG) was determined to be in the range of 0.45 to 0.13 from 450 to 700 °C; 0.45 to 0.13 for sub-bituminous (SUB); 0.42 to 0.09 for light volatile bituminous (BIT-LV); 0.45 to 0.14 for high volatile bituminous; 0.40 to 0.13 for semi-anthracite (SA); and 0.31 to 0.13 for the anthracite (ANT). There was a convergence of the atomic H/C ratio at a temperature of 700 °C (char forming temperature) for all the heated treated coals. The atomic O/C ratio for LIG was determined to be in the range of 0.10 to 0.02; 0.08 to 0.03 for SUB; 0.05 to 0.03 for BIT-LV; 0.05 to 0.01 for BIT-HV; 0.04 to 0.03 for SA; and 0.03 for ANT. This variation in the values of the atomic O/C ratio with decreasing coal rank with heat treatment can

be explained from the petrographic composition of the coal as can be seen in Table 2. The porosity increased with increasing pyrolysis temperature to a maximum at 650 °C, thereafter there was a drop in the porosity. The porosity was obtained to be in the range of 13 to 22 % for LIG from 450 to 650 °C; 11 to 20 % for SUB; 11 to 20 for BIT-LV; 12 to 23 for BIT-HV; 14 to 23 for SA; and 11 to 21 for ANT. The same trend was observed for the calorific value of the coal chars as reflected in Table 2. This implies that the maximum temperature to get the heat effect of coal is 650 °C. The aromaticity was observed to increase with increasing pyrolysis temperature, a trend that is generally consistent with previous reports on coal systems in that the lignite has the lowest values and the anthracite the highest values (Odeh, 2015). The fuel ratio demonstrated same trend as the aromaticity as the values determined increased with increasing pyrolysis temperature. A convergence to almost the same value was observed for the fuel ratio most especially for the low rank to medium rank coals around 700 °C. The surface area was observed to increase with increase in the pyrolysis temperature with the low rank coals exhibiting values while the rank exhibited the least value. The results relating to the volatile release was considered in terms of the decomposition of oxygen-containing functional groups and hydrogen-containing functional groups, coupled with the increase in the carbon content attributed to the structural re-arrangement of the aromatic structures of the coal which could lead to swelling and increase in porosity (Odeh et al., 2017).

### 3.3. Assessment of the O<sub>2</sub> Combustion Reactivity of Chars

Table 4 gives a comprehensive summary of detailed O<sub>2</sub> combustion reactivity analysis, where chars are listed by increasing coal rank (lignite to anthracite).

Table 4: Specific and intrinsic reactivity of chars

| Char      | Rs (g/gs)         | R <sub>I</sub> (g/m <sup>2</sup> s) | Rs (g/gs)         | R <sub>I</sub> (g/m <sup>2</sup> s) | Rs (g/gs)         | R <sub>I</sub> (g/m <sup>2</sup> s) | Rs (g/gs)         | R <sub>I</sub> (g/m <sup>2</sup> s) |
|-----------|-------------------|-------------------------------------|-------------------|-------------------------------------|-------------------|-------------------------------------|-------------------|-------------------------------------|
|           | x10 <sup>-5</sup> | x10 <sup>-7</sup>                   | x10 <sup>-5</sup> | x10 <sup>-7</sup>                   | x10 <sup>-5</sup> | x10 <sup>-7</sup>                   | x10 <sup>-5</sup> | x10 <sup>-7</sup>                   |
| C/Temp    | 415 °C            |                                     | 400 °C            |                                     | 385 °C            |                                     | 370 °C            |                                     |
| LIG450    | 7.42              | 2.61                                | 7.20              | 2.53                                | 6.22              | 2.19                                | 7.91              | 2.78                                |
| LIG500    | 8.07              | 2.47                                | 6.17              | 1.89                                | 6.98              | 2.13                                | 8.77              | 2.68                                |
| LIG550    | 7.70              | 2.02                                | 6.85              | 1.80                                | 5.83              | 1.53                                | 6.95              | 1.82                                |
| LIG600    | 6.15              | 1.48                                | 5.90              | 1.42                                | 5.99              | 1.45                                | 5.23              | 1.26                                |
| LIG650    | 5.58              | 1.24                                | 5.57              | 1.24                                | 6.31              | 1.40                                | 7.95              | 1.76                                |
| LIG700    | 4.42              | 0.93                                | 3.84              | 0.81                                | 3.78              | 0.80                                | 3.41              | 0.72                                |
| SUB450    | 7.85              | 3.19                                | 7.18              | 2.92                                | 6.75              | 2.74                                | 8.99              | 3.65                                |
| SUB500    | 7.21              | 2.48                                | 6.83              | 2.35                                | 6.15              | 2.17                                | 7.27              | 2.50                                |
| SUB550    | 7.13              | 2.44                                | 6.68              | 2.29                                | 6.32              | 2.11                                | 8.25              | 2.83                                |
| SUB600    | 6.82              | 1.76                                | 6.78              | 1.75                                | 6.54              | 1.69                                | 8.05              | 2.08                                |
| SUB650    | 6.61              | 1.63                                | 5.72              | 1.41                                | 5.60              | 1.38                                | 6.37              | 1.57                                |
| SUB700    | 6.25              | 1.51                                | 4.90              | 1.18                                | 5.22              | 1.26                                | 7.84              | 1.90                                |
| BIT-LV450 | 8.03              | 3.31                                | 7.62              | 3.14                                | 7.42              | 3.06                                | 8.43              | 3.47                                |
| BIT-LV500 | 7.01              | 2.77                                | 7.10              | 2.81                                | 6.91              | 2.73                                | 8.35              | 3.30                                |
| BIT-LV550 | 6.95              | 2.09                                | 6.94              | 2.08                                | 6.83              | 2.05                                | 7.15              | 2.15                                |
| BIT-LV600 | 6.79              | 2.01                                | 6.27              | 1.85                                | 6.61              | 1.95                                | 7.49              | 2.22                                |
| BIT-LV650 | 6.41              | 1.71                                | 5.63              | 1.75                                | 6.06              | 1.62                                | 6.23              | 1.67                                |
| BIT-LV700 | 5.70              | 1.42                                | 5.92              | 1.47                                | 6.17              | 1.53                                | 5.88              | 1.46                                |
| BIT-HV450 | 6.74              | 3.27                                | 6.04              | 2.93                                | 5.58              | 2.71                                | 8.19              | 3.98                                |
| BIT-HV500 | 6.50              | 2.57                                | 5.49              | 2.17                                | 5.82              | 2.30                                | 6.30              | 2.49                                |
| BIT-HV550 | 6.48              | 2.21                                | 5.34              | 1.82                                | 5.68              | 1.93                                | 6.28              | 2.14                                |
| BIT-HV600 | 5.74              | 1.73                                | 5.31              | 1.90                                | 5.50              | 1.66                                | 5.50              | 1.66                                |
| BIT-HV650 | 5.11              | 1.47                                | 4.75              | 1.37                                | 4.77              | 1.38                                | 5.18              | 1.50                                |
| BIT-HV700 | 5.27              | 1.46                                | 4.04              | 1.12                                | 3.35              | 0.93                                | 2.29              | 0.64                                |
| SA450     | 6.16              | 2.78                                | 4.38              | 1.98                                | 4.25              | 1.92                                | 4.24              | 1.91                                |
| SA500     | 5.66              | 2.38                                | 4.37              | 1.84                                | 3.81              | 1.60                                | 3.88              | 1.63                                |
| SA550     | 4.48              | 1.64                                | 3.62              | 1.33                                | 2.99              | 1.56                                | 4.44              | 1.62                                |
| SA600     | 4.79              | 1.60                                | 3.70              | 1.23                                | 4.27              | 1.00                                | 2.06              | 0.69                                |
| SA650     | 4.76              | 1.52                                | 3.52              | 1.12                                | 2.22              | 0.71                                | 2.94              | 0.94                                |
| SA700     | 3.15              | 0.86                                | 2.61              | 0.71                                | 0.90              | 0.25                                | 1.85              | 0.50                                |
| ANT450    | 4.31              | 1.95                                | 2.87              | 1.49                                | 2.63              | 1.30                                | 1.23              | 0.56                                |
| ANT500    | 3.62              | 1.73                                | 2.21              | 1.05                                | 2.05              | 0.98                                | 0.87              | 0.42                                |
| ANT550    | 3.01              | 1.38                                | 1.70              | 0.78                                | 1.75              | 0.80                                | 0.43              | 0.20                                |
| ANT600    | 2.59              | 1.08                                | 1.53              | 0.64                                | 1.06              | 0.44                                | 0.29              | 0.12                                |
| ANT650    | 2.40              | 0.92                                | 1.51              | 0.58                                | 0.35              | 0.13                                | 0.49              | 0.19                                |
| ANT700    | 2.04              | 0.77                                | 1.13              | 0.43                                | 0.32              | 0.12                                | 0.49              | 0.19                                |

C/TEMP=combustion temperature; R<sub>S</sub>=specific reactivity; R<sub>I</sub>=intrinsic reactivity

The results for the specific reactivity of the chars were consistent with decreasing trend of reactivity with increasing combustion temperature (excluding 370 °C for the low and medium rank coals). Therefore, the specific reactivity was determined to be in the range of 4.24 to 6.16 x 10<sup>-5</sup> g/g.s for SA450 and 1.23 to 4.31 x 10<sup>-5</sup> g/g.s for ANT450 from a combustion temperature of 370 to 415 °C. Similar trends were obtained for all the chars prepared at the other temperatures. The irregular and random distribution of the specific reactivity with increasing temperature at which chars were obtained can be attributed to the variation in petrographic composition as can be seen in Table 2. To correct this irregular phenomenon noticed with the specific reactivity, the specific reaction rate data were normalized to the measured CO<sub>2</sub> adsorption DR (Dubinin-Radushkevich) surface area (Table 3) (Odeh, 2015). Roberts and Harris (2007) has reported that normalizing the specific reactivity with the DR surface area makes room for intrinsic reaction rate and allows for a more useful comparison of the actual char-gas reaction kinetics, hence correcting the random trend experienced with the specific reactivity data (Roberts and Harris, 2007). Similar trends were also exhibited by all the other chars used in this investigation for the different coal suites. Also observed was the decreasing trend of the intrinsic reactivity with increasing pyrolysis temperature (temperature at which chars was obtained). For instance, at a combustion temperature of 415 °C, the intrinsic reactivity was obtained in the range of 2.61 to 0.93 x 10<sup>-7</sup> g/m<sup>2</sup> s for LIG from 450 to 700 °C; 3.19 to 1.51 x 10<sup>-7</sup> g/m<sup>2</sup> s for SUB; 3.31 to 1.42 x 10<sup>-7</sup> g/m<sup>2</sup> s for BIT-LV; 3.27 to 1.46 x 10<sup>-7</sup> g/m<sup>2</sup> s for BIT-HV; 2.78 to 0.86 x 10<sup>-7</sup> g/m<sup>2</sup> s for SA and 1.95 to 0.77 x 10<sup>-7</sup> g/m<sup>2</sup> s for ANT respectively. The decrease of reactivity with increasing pyrolysis temperature has been reported to be due to the reduction of the hydrogen content in chars which is related to the reduction of active sites giving room for more desorption reaction with oxygen (Odeh et al., 2017). From a qualitative point of view and considering the lowest pyrolysis temperature of 450 °C, the data suggests that the medium rank coals are more reactive than the low and high rank coals. Based on this presumption, the reactivity order of the examined coals may be presented as:

$$\text{BIT-LV} > \text{BIT-HV} > \text{SUB} > \text{SA} > \text{LIG} > \text{ANT}$$

As can be seen, though the reactivity values seem to be close, this order of reactivity did not correlate with the coal rank. Generally, logical consideration and evaluation of the trend of the physical and chemical properties of the coals and chars in Table 1 and 3 would lead to the assessment of the reactivity and a suggestion, that the low-rank coal, lignite would be the most reactive and the order of reactivity may have been presented as:

$$\text{LIG} > \text{SUB} > \text{BIT-LV} > \text{BIT-HV} > \text{SA} > \text{ANT}$$

That is not the case in this investigation as the order of reactivity did not correlate with coal rank. These finding can be attributed to the fact that the coals were acid-washed and the impact was mostly felt in the low-rank coals (lignite and sub-bituminous] as revealed in this study and reported by Odeh (2005) and also by other investigators (Kulaots et al., 2007). Kulaots et al. (2007) reported that inherent minerals in the low rank coals do have favourable catalytic effects during coal processing. These inherent minerals would have been removed in the course of the acid- washing in this study. These minerals are mostly found in clay minerals (calcite and dolomite) consisting of aluminium oxides and oxides of calcium and potassium which plays active role in the de-alkylation and dehydrogenation reaction at high pyrolysis temperatures and in the cracking (decarboxylation/decarbonylation reactions) of oxygen functional groups at low pyrolysis temperatures (Odeh et al., 2017).

For a more quantitative understanding of this investigation, the activation energy, which is a temperature predominant parameter of the intrinsic reaction rate, was determined. The activation energy is found to vary dramatically over the course of the combustion analysis, exhibiting a sharp maximum in the early stages of char combustion. This dramatic behaviour can be attributed to the fact that when coal is heated, two processes occur competitively: one is the depolymerization process through which gas, water vapour and tar are formed and the other is the condensation or re-polymerization which leads to char formation. Relating the report of



Kulaots et al. (2007) to this investigation, chars prepared at temperatures less than 500 °C would have experienced depolymerization process which involves the breaking of bonds that requires a lot more energy than the condensation process, hence the higher activation energy exhibited in the early stages of the combustion process. Kulaots et al. (2002) has reported that chemical bonds in coal breaks easily at higher temperatures, which implies that the combustion reaction at higher temperature prepared chars will take place at lower activation energies.

Employing the data of the mean activation energy in conjunction with Fig.1, the order of reactivity may as well be now presented as:

BIT-LV > SA > BIT-HV > ANT > SUB > LIG

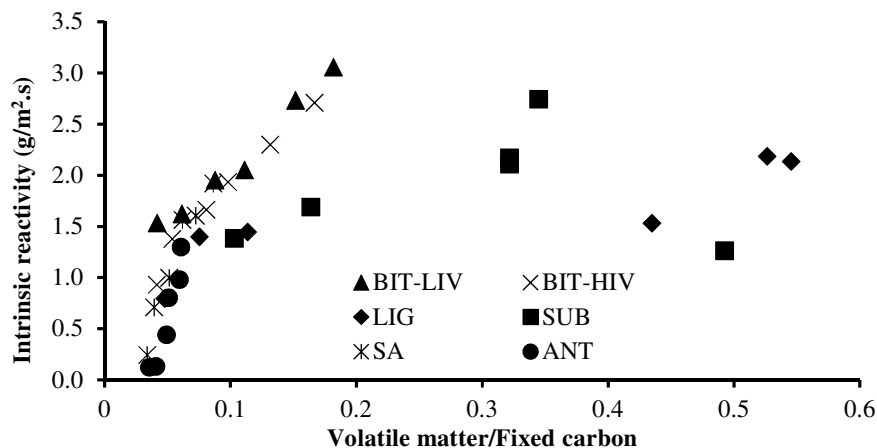


Figure 1: Plot of intrinsic reactivity versus inverse of fuel ratio

#### 4. CONCLUSION

The results presented in this work show the characterization of six acid-washed coals of different ranks and the impact of the changes (chemical, physical and optical) on the resultant char reactivities. The chemical and physical properties of the chars at six different pyrolysis temperatures were obtained using both conventional and advanced analytical techniques, while the optical properties were obtained from detailed petrographic analysis. All the different ranks of coal show similar chemical and physical properties behaviour in char properties and the order of the determined characteristics is found consistent with the ranks of the coal. However, the order of intrinsic reactivity does not correlate with the coal rank as presumed based on the physical and chemical properties as the medium rank coals were found to be more reactive than the other ranks of coal. This revelation was only possible through acid cleaning of coal which is a vital process in clean coal technology and as such the authors see this as a novelty in clean coal processes. Moreover, this presumption was corrected when the petrographic data was included in the correlation, implying that not only chemical and physical properties but also petrographic properties (maceral content distribution) do play an important role in the reactivity behaviour of coals.

#### 5. CONFLICT OF INTEREST

There is no conflict of interest associated with this work.

**REFERENCES**

- Aarna, I. and Suuberg, E.M. (1998). Changes in reactive surface area and porosity during char oxidation. *Symposium on Combustion/The Combustion Institute*, 27, pp. 2933 – 2939.
- Arenillas, A., Pevida, C., Rubiera, F. and Pis, J.J. (2003). Comparison between the reactivity of coal and synthetic coal models. *Fuel*, 82, pp. 2001-2006.
- Bar-Ziv, E. and Kantorovich, I.I. (2001). Mutual effects of porosity and reactivity in char oxidation. *Progress in Energy and Combustion Science*, 27, pp. 667 – 697.
- Beamish, B., Shaw, K.J., Rodgers, K.J. and Newman, J. (1998). Thermogravimetric determination of the carbon dioxide reactivity of char from some New Zealand coals and its association with the inorganic geochemistry of the parent coal. *Fuel Processing Technology*, 53, pp. 243 – 253.
- Jones, J.M., Pourkashanian, M., Rena, C.D. and Williams, A. (1999). Modelling the relationship of coal structure to char porosity. *Fuel*, 78, pp. 1737 – 1744.
- Kulaots, I., Aarna, I., Callejo, M., Hurt, R.H. and Suuberg, E.M. (2002). Development of porosity during coal char combustion. *Proceedings of the Combustion Institute*, 29, pp.495 – 501.
- Kulaots, I., Hsu, A. and Suuberg, E.M. (2007). The role of porosity in char combustion. *Proceedings of the Combustion Institute*, 31, pp. 1897 – 1903.
- Liu, G., Benyon, P., Benfell, K.E., Bryant, G.W., Tate, A.G., Boyd, R.K., Harris, D.J. and Wall, T.F. (2000). The porous structure of bituminous coal chars and its influence on combustion and gasification under chemically controlled conditions. *Fuel*, 79, pp. 617 – 626.
- Sima-Ella, E., Yuan, G. and Mays, T. (2005). A simple kinetic analysis to determine the intrinsic reactivity of coal chars. *Fuel*, 84, pp. 1920 – 1925.
- Odeh, A. (2015). Exploring the potential of petrographics in understanding coal pyrolysis. *Energy*, 87, pp. 555 – 565.
- Odeh, A.O., Ogebeide, S.E. and Okieimen, C.O. (2017). Coal pyrolysis: Comparative evaluation of the technical performance of two Southern Hemisphere demineralized bituminous coals. *Thermal Science and Engineering Progress*, 3, pp. 1 – 9.
- Roberts, D.G. and Harris, D.J. (2007). Char gasification in mixtures of CO<sub>2</sub> and H<sub>2</sub>O: competition and inhibition. *Fuel*, 86, pp. 2672-2678.